International Journal of Pharmaceutics 625 (2022) 122132

Contents lists available at ScienceDirect

International Journal of Pharmaceutics

journal homepage: www.elsevier.com/locate/ijpharm

In vivo investigation of Gallium-68 and Bismuth-205/206 labeled beta cyclodextrin for targeted alpha therapy of prostaglandin E2 receptor-expressing tumors in mice

Katalin Csige [a,b], Judit P. Szabó [a], Ibolya Kálmán-Szabó [a], Noémi S. Dénes [a], Dezső Szikra [a], Zita Képes [a], Gábor Opposits [a], Gábor Méhes [c], István Kertész [a], Ferenc Fenyvesi [d], György Trencsényi [a,1], István Hajdu [a,b,1,*]

[a] Division of Nuclear Medicine and Translational Imaging, Department of Medical Imaging, Faculty of Medicine, University of Debrecen, Nagyerdei St. 98, H-4032 Debrecen, Hungary
[b] Doctoral School of Pharmaceutical Sciences, University of Debrecen, Nagyerdei St. 98, H-4032 Debrecen, Hungary
[c] Department of Pathology, Faculty of Medicine, University of Debrecen, Nagyerdei St. 98, H-4032 Debrecen, Hungary
[d] Department of Pharmaceutical Technology, Faculty of Pharmacy, University of Debrecen, Nagyerdei St. 98, H-4032 Debrecen, Hungary

ARTICLE INFO

Keywords:
Radiotherapy
Cyclodextrin
Targeted alpha therapy
Prostaglandin E2
Pancreas adenocarcinoma

ABSTRACT

Prostaglandin E2 (PGE2) molecule and its receptors play an important role in the development of malignancies and metastases therefore PGE2 may play a crucial role in the diagnosis and a new therapeutic target in the field of radionuclide therapy of PGE2-positive tumors. PGE2 form complexes with RAMEB (randomly-methylated-beta-cyclodextrin) with high affinity therefore the aim of this present study was to synthesize a PGE2-specific DOTAGA-RAMEB, which can be labeled with diagnostic and therapeutic isotopes also and binds to PGE2-positive tumors. DOTAGA-RAMEB was labeled with ^{68}Ga and $^{205/206}$Bi radionuclides and their radiochemical purity (RCP%), partition coefficient (log*P* values), and *in vitro* and *in vivo* stability were determined. For the assessment of the biological properties and the PGE2 specificity of [^{68}Ga]Ga-DOTAGA-RAMEB and [$^{205/206}$Bi]Bi-DOTAGA-RAMEB *in vivo* PET imaging and *ex vivo* biodistribution studies were performed using healthy control and PGE2-positive BxPC-3 tumor-bearing CB17 SCID mice. The RCP% of the newly synthesized [^{68}Ga]Ga-DOTAGA-RAMEB and [$^{205/206}$Bi]Bi-DOTAGA-RAMEB was higher than 98 %. *In vivo* studies showed that the tumor-to-background ratio of [^{68}Ga]Ga-DOTAGA-RAMEB was 2.5 ± 0.2 as a result BxPC-3 tumors were clearly identified on PET images. Beside this the *ex vivo* biodistribution studies showed that the accumulation rate of [^{68}Ga]Ga-DOTAGA-RAMEB and [$^{205/206}$Bi]Bi-DOTAGA-RAMEB was similar in the PGE2-positive BxPC-3 tumors.

1. Introduction

Given the staggering global prevalence malignant diseases impose on societies, there is an increasing interest for the introduction of sensitive imaging modalities and therapeutical possibilities that excel in the timely detection and treatment of functional neoplastic alterations prior to apparent morphological changes. In the diagnostic and therapeutic settings of neoplastic diseases nuclear medicine may not fall short here, as we have much to offer.

PGE2 play a pivotal role in tumor niche, its receptors seem to be promising novel anti-tumor therapeutic targets in cancer management (Reader et al., 2011; Tong et al., 2018). Further, they may be valuable prognostic biomarkers in the follow-up of malignant diseases and represent diagnostic tumor-related targets in *in vivo* nuclear medical molecular imaging. For this purpose, one of the most promising pharmaceutical candidate groups are the cyclodextrins.

Cyclodextrins are polymers composed of cyclic oligosaccharides of truncated cone shape or toroids. According to their chemical structure they can be divided into three main groups. Typical cyclodextrins contain 6, 7, or 8 glucose units and are denoted α-, β-, and γ-cyclodextrins, respectively. They have a hydrophilic exterior surface and a

* Corresponding author at: Division of Nuclear Medicine and Translational Imaging, Department of Medical Imaging, Faculty of Medicine, University of Debrecen, Debrecen, Hungary.
E-mail address: hajdu.istvan@med.unideb.hu (I. Hajdu).
[1] These authors contributed equally to this study.

https://doi.org/10.1016/j.ijpharm.2022.122132
Received 2 May 2022; Received in revised form 26 July 2022; Accepted 18 August 2022
Available online 24 August 2022

Abbreviations

DIPEA	N,*N*-Diisopropylethylamine
DOTA	1,4,7,10-tetraazacyclododecane-1,4,7,10-tetraacetic acid
DOTAGA	p-NCS-Bz-DOTA-GA, (2,2′,2″-(10-(1-carboxy-4-((4-isothiocyanatobenzyl)amino)-4-oxobutyl)-1,4,7,10-tetraazacyclododecane-1,4,7-triyl)triacetic acid)
DTPA	diethylene triamine pentaacetic acid
EP	E-type prostanoid receptor
HPβCD	(2-Hydroxypropyl)-β-cyclodextrin
i.v.	intravenous(ly)
LET	linear energy transfer
log*P*	octanol – water partition coefficient
MS	mass spectrometer
Mw	molecular weight
NODAGA	p-NCS-benzyl-NODA-GA
PET	positron emission tomography
PGE2	prostaglandin E2
RAMEB	randomly methylated β-cyclodextrin
RCP	radiochemical purity
RCY	radiochemical yield
RP-HPLC	reversed-phase high-performance liquid chromatography
TAT	targeted alpha therapy
TRIS	2-Amino-2-(hydroxymethyl)-1,3-propanediol
u.p	ultra-pure

hydrophobic interior cavity, enabling them to form host–guest inclusion complexes with a wide range of pharmaceuticals in aqueous solution. A great number of chemically modified cyclodextrins have been prepared recently to enhance the complexation capacity and the physicochemical properties. Cyclodextrins are commonly used excipients in pharmaceutical formulations for increasing the bioavailability of hydrophobic drugs. In addition, some of their varieties such as 2-Hydroxypropyl-beta-cyclodextrin (HPBCD) also applied as an orphan drug for the treatment of Niemann-Pick disease, type C (Ottinger et al., 2014). The Food and Drug Administration generally recognizes cyclodextrins as safe when used to increase bioavailability of drugs. Despite of the intensive research, limited information is available on the pharmacokinetic and biodistribution of cyclodextrins. Most studies focused on the toxicity only. For this reason our research group started to investigate the pharmacokinetic properties of cyclodextrins using a sensitive non-invasive positron emission tomography (PET) We published for the first time the whole body dynamic biodistribution study of the newly synthetized Gallium-68-labeled NODAGA-hydroxypropyl-beta-cyclodextrin ([^{68}Ga]Ga-NODAGA-HPBCD) (Hajdu et al., 2019). In that paper, we focused on the radiochemical synthesis, biodistribution and pharmacokinetic properties of the [^{68}Ga]Ga-NODAGA-HPBCD using dynamic and static PET technique. The *in vitro* experiments demonstrated that the [^{68}Ga]Ga-NODAGA-HPBCD similarly to earlier published results is highly hydrophilic (Del Valle, 2004) and therefore it was mainly excreted through the urinary system fast, similar to unlabeled HPBCD (Frijlink et al., 1990) To better understand the pharmacokinetic, biodistribution and the exact mechanism of action of cyclodextrins at the level of tissues and cells our research group further investigated the ^{68}Ga labeled cyclodextrin derivatives. It was earlier reported that randomly methylated β-cyclodextrin (RAMEB) show a high affinity to form complexes with prostaglandin E2 (PGE2). The PGE2 receptors play crucial role in inflammation, and carcinogenesis, therefore PGE2 is a novel and intensively investigated molecular target in anticancer therapy (O'Callaghan and Houston, 2015; Reader et al., 2011; Tong et al., 2018). In our recently published report we issued the radiochemical synthesis, pharmacokinetic properties biodistribution and tumor accumulation of the ^{68}Ga-labeled RAMEB (Trencsényi et al., 2020). The *in vivo* PET studies demonstrated that [^{68}Ga]Ga-NODAGA-RAMEB was mainly excreted through the urinary system, and uptake of the abdominal and thoracic organs and tissues was low. Specific uptake of [^{68}Ga]Ga-NODAGA-RAMEB was observed only in the tumor. First time was confirmed *in vivo* that the Gallium-68 labeled cyclodextrin derivative accumulates specifically in the PGE2 receptors overexpressing tumor.

The aims of present study were to synthetize and *in vivo* investigate the PGE2 specific DOTAGA-RAMEB which cyclodextrin-based molecule is suitable for the targeted alpha therapy (TAT). TAT using alpha emitters has shown great promise in the treatment of tumors in preclinical and clinical studies (Kratochwil et al., 2014; Norenberg et al., 2006). Alpha emitting radionuclides emit high linear energy transfer (LET) α-particles, within a relative short range (<100 μm). Based on the decay properties only a limited number of alpha-emitting radioisotopes are suitable for radiotherapy, such as ^{211}At, ^{213}Bi, ^{225}Ac, ^{223}Ra, ^{212}Pb, ^{227}Th, or ^{149}Tb. The half-life of the radionuclide is a critical factor in therapeutic applications; it should not be too short to allow enough time for radiochemical synthesis, and administration to the patient, and should not be too long to avoid too high patient dose (Nelson et al., 2020). Another important point that the biological half-life of the carrier should be compatible with the physical half-life of the radioisotope. In the general approach, radionuclide with shorter half-life is a much better match with carrier molecules that have a short biological half-life, such as small molecules, peptides, or antibody fragments (Ahenkorah et al., 2021; Kellerbauer et al., 2020). Based on these considerations the generator derived radionuclide Bismuth-213 (^{213}Bi, $T_{1/2}$ = 46 min) was selected for this research project. Due to the short range and high linear energy transfer (LET ≈ 100 keV/μm) of alpha particles ^{213}Bi can deliver a high radiation dose rate to the target within a short period of time. Moreover ^{213}Bi is available from ^{225}Ac/^{213}Bi radionuclide generator systems and is comfortably produced in house before application (Morgenstern et al., 2012). The advantageous chemical characteristics of Bi(III) (trivalent metal ion) allow the stable linking to biomolecules using chelators: DOTA and DTPA. These physical properties make ^{213}Bi, one of the most commonly used α-emitting radionuclides for medical applications. In our experiments $^{205/206}$Bi isotopes produced in our institute (as surrogates of α-emitting ^{213}Bi) were used for radiolabeling of DOTAGA-RAMEB. Due to the longer half-lives [^{205}Bi ($t_{1/2}$ = 15.3 days) and ^{206}Bi ($t_{1/2}$ = 6.24 days)] $^{205/206}$Bi is suitable for the development of the model compound under preclinical conditions.

In this work, we describe the conjugation of DOTA derivative DOTAGA anhydride bifunctional chelating agents to a randomly methylated β-cyclodextrin. Radiolabeling of DOTAGA-RAMEB conjugate with gallium-68 and bismuth-205/206 isotopes was performed, optimized and characterized, and the *in vivo* behavior of this radiotracers was evaluated in a model of PGE2-expressing human pancreatic adenocarcinoma-bearing mouse model.

2. Materials and methods

2.1. Chemicals

6-Monodeoxy-6-monoamino-randomly-methylated-beta-cyclodextrin hydrochloride (NH_2-RAMEB) was the product of CycloLab ltd. (Budapest, Hungary). p-NCS-Bz-DOTA-GA (DOTAGA) was purchased from CheMatech (Cat. No.:C115) (Dijon, France). Ultrapure water (Sigma-Aldrich Kft., Budapest, Hungary) was used for preparing every solvent and mixture during this research work. When metal-free conditions were needed, glassware was washed with HCl and rinsed with Milli-Q ultrapure water. The *N,N* Diisopropylethylamine (DIPEA), 2-Amino-2-(hydroxymethyl)-1,3-propanediol (TRIS base) and ascorbic

acid was acquired from Sigma-Aldrich Kft. (Budapest, Hungary). Ultrapure hydrochloric acid (u.p. HCl) was purchased from Merck Kft. (Budapest, Hungary). All other chemicals were obtained from Sigma-Aldrich Kft. (Budapest, Hungary) and VWR International Kft. (Debrecen, Hungary) and were used without further purification.

2.2. Conjugation of DOTAGA to NH_2-RAMEB

DOTAGA bifunctional chelator was conjugated via the amino group of NH_2-RAMEB based on the protocol as described earlier (Hajdu et al., 2019; Trencsényi et al., 2020). Briefly, 10 mg (8 μM) NH_2-RAMEB was dissolved in 1.5 mL water and the solution was cooled and stirred for 15 min. 5.5 mg (8 μM) DOTAGA was added to the cooled NH_2-RAMEB solution, and the pH of the reaction mixture was adjusted to 8.5 by adding DIPEA dropwise. The reaction mixture was stirred at room temperature for 24 h. The product (DOTAGA-RAMEB) was lyophilized, re-dissolved in water and purified on a Knauer HPLC system using a Supelco Discovery® BIO Wide Pore semi preparative C-18 column (150 mm × 10 mm, particle size: 10 μm). Detection was performed using a Waters absorbance detector at 254 nm, and the flow rate of the gradient elution was 4 mL/min. The mobile phase was composed of solvent A (0.1 % formic acid in water) and solvent B (acetonitrile–water (95:5, v/v)). The gradient of solvent A started with 90 % to 90 % at 2 min to 20 % at 30 min. Synthesis yield was 77 %. In order to verify the purity of the precursor DOTAGA-RAMEB, a KNAUER RP-HPLC system with Supelco Discovery® Bio Wide Pore C-18 column (250 mm × 4.6 mm; particle size: 10 μm) was used. Signals were detected using a KNAUER absorbance detector at 254 nm and the gradient elution was achieved at a flow rate of 1 mL/min. The mobile phase 0.1 % formic acid in water (solvent A) and acetonitrile–water (95:5, v/v) (solvent B). The gradient was programmed as follows: solvent A started with 100 % to 10 % at 15 min to 10 % at 17 min to 100 % at 20 min. Molecular weight was confirmed with high-resolution mass spectrometry (MS) (maXis II UHR ESI-TOF MS, Bruker Corp. Billerica, Massachusetts, USA). In the last step, 3 mM stock solution was prepared from the product (DOTAGA-RAMEB) in ultra-pure water for the radiolabeling reactions.

2.3. [^{68}Ga]Ga-DOTAGA-RAMEB radiolabeling

^{68}Ga ($t_{½}$ = 68 min, β+ = 89 % and EC = 11 %) was available from a ^{68}Ge/^{68}Ga generator system (50 mCi, Gallia-Pharm, Eckert and Ziegler Germany). The ^{68}Ga was eluted with 5 mL of 0.1 M u.p. HCl. The generator eluate was fractioned by discarding the first 1.6 mL and collecting the next 1–1.2 mL for the synthesis. The top fraction contained 70–75 % of the total radioactivity. 1 mL from the collected ^{68}Ga eluate was buffered with sodium acetate (1 M, 160 μL) to ensure a pH of 4.3–4.5 in a 5 mL Eppendorf tube. Thereafter, an aqueous solution of DOTAGA-RAMEB (3 mM, 5 μL) was added. The reaction was conducted by applying conventional heating at 95 °C for 10 min. Afterward the solution was pipetted into a Light C18 Sep-Pak Cartridge and was washed with 2 mL of water. The ^{68}Ga labeled product ([^{68}Ga]Ga-DOTAGA-RAMEB) was eluted with 400 μL mixture of 96 % EtOH/isotonic NaCl solution. In order to evaluating the radiochemical purity, the above-mentioned KNAUER RP-HPLC system was used with the Supelco Discovery® Bio Wide Pore C-18 analytical column (250 mm × 4.6 mm; particle size: 10 μm). The HPLC system was combined with radio detector and the signals were detected by both radio and absorbance detector simultaneously. Before using for animal experiments the product was sterile filtered and diluted with isotonic (0.9 %) saline solution.

2.4. Production and purification of $^{205/206}$Bi Isotopes.

The $^{205/206}$Bi isotope mixture was produced in a GE PETtrace cyclotron at the Division of Nuclear Medicine and Translational Imaging, Department of Medical Imaging, University of Debrecen with 16 MeV beam on natural Pb-foil target as described earlier (Manna et al., 2020). After a 60 min irradiation and a 24 h decay period, the irradiated Pb target was dissolved in u.p. HNO_3 (7 M, 2 mL). The solution was concentrated to ~1 mL, and was separated from the solid precipitation and diluted to 10 mL with water. This $^{205/206}$Bi isotope containing solution was transferred onto a preconditioned TK 200 resin (150 mg) column. After the loading of solution, the column was washed with u.p. HNO_3 (0.7 M, 5 mL) to remove the remaining Pb target materials, and the $^{205/206}$Bi isotopes were eluted with u.p. HNO_3 (7 M, 2 mL). The pure eluate which contained $^{205/206}$Bi isotopes (~30 MBq) were evaporated to dryness and were redissolved in u.p. HCl (0.1 M, 300 μL).

2.5. [$^{205/206}$Bi]Bi-DOTAGA-RAMEB radiolabeling

For the radiolabeling $^{205/206}$Bi solution (100 μL, 10 ± 0.8 MBq) was diluted to 300 μL with u.p. HCl (0.1 M) and was added to DOTAGA-RAMEB (3 mM, 10 μL) in a reaction vial including TRIS buffer (2 M, 50 μL) and ascorbic acid (20 %, 25 μL) at pH 8.4. The reaction was heated to 95 °C and incubated for 10 min and cooled to ambient temperature for 2 min. Afterward the solution was transferred to an Oasis HLB Extraction Cartridge (Waters Kft. Budapest, Hungary) and was washed with 2 mL of water. The $^{205/206}$Bi labeled product ([$^{205/206}$Bi]Bi-DOTAGA-RAMEB) was eluted with 200 μL mixture of 96 % EtOH/isotonic NaCl solution. In order to evaluating the radiochemical purity, the above-mentioned KNAUER RP-HPLC system was used with the Supelco Discovery® Bio Wide Pore C-18 analytical column (250 mm × 4.6 mm; particle size: 10 μm). The HPLC system was combined with radio detector and the signals were detected by both radio and absorbance detector simultaneously. Before using for animal experiments the product was sterile filtered and diluted with isotonic (0.9 %) saline solution. The product was diluted with saline solution and sterile filtered before animal experiments.

2.6. Determination of partition coefficient

The partition coefficient (log*P* values) of ^{68}Ga and $^{205/206}$Bi labeled DOTAGA-RAMEB were determined in separate experiments. [^{68}Ga]Ga-DOTAGA-RAMEB (10 μL, 5 ± 0.5 MBq) and [$^{205/206}$Bi]Bi-DOTAGA-RAMEB (10 μL, 4 ± 0.6 MBq) were diluted to 500 μL with PBS solution separately. These solutions were mixed with 500–500 μL of 1-octanol. The samples were stirred at room temperature for 20 min and then centrifuged at 20.000 rpm/min for 5 min at 4 °C for complete separation of the layers. 100 μL of samples were taken from the separated layers and were placed into test tubes. The radioactivity of the aliquots were measured with a Perkin-Elmer Packard Cobra gamma counter.

2.7. Determination of in vitro and in vivo metabolic stability

The *in vitro* stability of [^{68}Ga]Ga-DOTAGA-RAMEB and [$^{205/206}$Bi]Bi-DOTAGA-RAMEB was tested in mouse serum separately. Samples of [^{68}Ga]Ga-DOTAGA-RAMEB (10 μL, 5 ± 0.5 MBq) and [$^{205/206}$Bi]Bi-DOTAGA-RAMEB (10 μL, 4 ± 0.6 MBq) were added to mouse serum and incubated at 37 °C without stirring. 50 μL samples from this mixture were measured and added into ice-cold abs. ethanol (50 μL) at specific time points (30, 60, and 90 min). The mixture was then centrifuged at 10,000 rpm for 5 min at 4° C. The supernatant was collected, diluted with water and evaluated by analytical radio-HPLC. *In vivo* metabolic stability was measured in healthy SCID mice. Samples of [^{68}Ga]Ga-DOTAGA-RAMEB (8 ± 0.5 MBq) and [$^{205/206}$Bi]Bi-DOTAGA-RAMEB (6 ± 0.4 MBq) were administered into mice via the tail vein, and urine samples were collected 60 min after injection. The resulting sample (50 μL) was mixed with ice-cold abs ethanol and centrifuged at 10,000 rpm for 5 min. The supernatant was also analyzed by analytical radio-HPLC. In both cases, the HPLC chromatograms were compared with the initial chromatograms of the radiotracer to detect the presence of any radioactive metabolites.

2.8. Experimental animals

For our *in vivo* imaging studies and *ex vivo* organ distribution studies, CB17 SCID immunodeficient male mice (12-week-old, were purchased from Innovo ltd, Hungary; n = 35) were used. The animals were housed in a sterile IVC cage system (Techniplast, Italy) with 52 ± 10 % humidity, at a temperature of 26 ± 3 °C. Illumination was performed with artificial, automatically controlled 12-hour cycles. Mice were fed ad libitum with sterile semi-synthetic diet (sterile VRF1 rodent feed; Akronom Kft., Budapest, Hungary) and sterile drinking water were available ad libitum to all animals. Laboratory animals were kept and treated in compliance with all applicable sections of the Hungarian Laws and regulations of the European Union, with the permission of the Ethics Committee for Animal Experiments of the University of Debrecen (license number: 8/2016 / DEMÁB).

2.9. Induction of tumor model

For the induction of tumor models, male CB17 SCID mice were anesthetized with a pet inhalation anesthesia machine (TEC3 Eickemeyer Research isoflurane vaporizer; Ghislandi és Társai Kft., Budapest, Hungary). The skin on the left shoulder area of the experimental animals was shaved and was disinfected. Thereafter BxPC-3 human pancreas adenocarcinoma cells (ATCC, CRL-168, kind gift from the University of Hamburg) (5×10^6 cells in 100 µL 0.9 % NaCl) were injected subcutaneously. *Ex vivo* and *in vivo* biodistribution studies were performed 12 ± 1 days after subcutaneous injection of tumor cells at the tumor volume of 98 ± 5 mm^3.

2.10. In vivo PET imaging

Healthy control and approximately 12 days after tumor cell inoculation, BxPC-3 tumor bearing mice were anesthetized with 3 % isoflurane (Forane) with a dedicated pet anesthetic device (Eickemeyer Research, Tec3, Ghislandi Kft., Hungary). After anesthesia the animals were injected with 6.4 ± 0.3 MBq [^{68}Ga]Ga-DOTAGA-RAMEB via the lateral tail vein. Following injections, *in vivo* static and dynamic (0–90 min) PET imaging were performed to determine the biodistribution of the radiotracer using a MiniPET-II dedicated small animal PET scanner under inhalation anesthesia.

2.11. Analysis of PET data

Ellipsoid 3-dimensional volumes of interest (VOI) were manually drawn around the edge of the organ activity by visual inspection using BrainCad image analysis software. To quantify the concentration of radioactivity in the tumors, organs and tissues standardized uptake value (SUV) was determined as follows: SUV = [VOI activity (Bq/mL)]/[injected activity (Bq)/animal weight (g)], assuming a density of 1 g/mL. Tumor-to-muscle (T/M) ratios were assessed from the SUVmean of tumor and SUVmean of the background (muscle).

2.12. Ex vivo organ distribution studies

For *ex vivo* biodistribution studies, control and tumor-bearing (BxPC-3) SCID mice were injected intravenously with 6.2 ± 0.2 MBq of [^{68}Ga]Ga-DOTAGA-RAMEB or 0.86 ± 0.17 MBq of [$^{205/206}$Bi]Bi-DOTAGA-RAMEB. 30, 60 and 90 min after injection of radiotracers, the animals were anesthetized with 5 % isoflurane. Three tissue samples were taken from selected organs and radioactivity and their weight were measured with a calibrated gamma counter (Perkin-Elmer Packard Cobra, Waltham, MA). Uptake of ^{68}Ga- and $^{205/206}$Bi-labeled DOTAGA-RAMEB was expressed in the mean values of the percent injected dose per gram (% ID/g) tissue.

2.13. Immunohistochemistry

This protocol is based on the procedure described by (Trencsényi et al., 2020) Shortly, four µm thick sections of formaldehyde-fixed and paraffin-embedded BxPC-3 xenograft tumors were treated with rabbit anti-prostaglandin E Receptor EP2/PTGER2 monoclonal antibody (Abcam, USA; catalog number: ab16717) at a dilution of 1:1000 after deparaffination and rehydration (pH = 6). An HRP-labeled anti-rabbit polymer antibody (Mach2, BioCare Medical, USA, Cat. No. RHRP520) and the Envision DAB detection Kit (DAKO-Agilent Technologies, USA) were used to detect and visualize the specific antibody binding. For counterstaining hematoxylin was applied. Microscopic images were taken with a Leica DM2500 research microscope equipped with a DFC495 digital camera and LAS imaging kit.

2.14. Statistical data processing

Statistical analyses were evaluated by two-way ANOVA, Student's *t*-test (two-tailed) and Mann-Whitney *U* test and the significance level was set at $p \leq 0.05$ unless otherwise indicated. All characterization experiments were performed in triplicates at the minimum and the data are presented as mean ± SD.

3. Results

3.1. Chemistry

A schematic illustration of the precursor synthesis is shown in Fig. 1A. The DOTAGA-RAMEB precursor was prepared by conjugation reaction of a primary amine containing RAMEB and DOTAGA bifunctional chelator. This modification allows the modified cyclodextrin derivative to be labeled with both ^{68}Ga and $^{205/206}$Bi radioisotopes. The final product was purified by HPLC and the purity was more than 98 % (Fig. 1B). The structure of DOTAGA-RAMEB was identified by high-resolution mass spectrometry (UHR ESI-TOF MS). Based on the MS measurement, the theoretical and measured mass of the synthesized products were in concordance, where the calculated mass of DOTAGA-RAMEB *m/z*: 1882.7721 $[M]^{1+}$ and the measured mass: 1882.7764 $[M]^{1+}$ (Fig. 1C).

3.2. Radiochemistry

^{68}Ga and $^{205/206}$Bi radiolabeling of the bifunctional chelator-modified cyclodextrin derivative (DOTAGA-RAMEB) was performed manually in both cases (Fig. 2A). The average reaction time of radiochemical labeling reactions was approximately 20 min. The radiochemical purity (RCP) of products was found over 98.0 % in both cases. (Fig. 2B and 2C).

3.3. Determination of partition coefficient and in vitro, in vivo metabolic stability

The log*P* value of [^{68}Ga]Ga-DOTAGA-RAMEB was −3.47 ± 0.04, and the log*P* value of [$^{205/206}$Bi]Bi-DOTAGA-RAMEB was −3.45 ± 0.03, which is indicating a hydrophilic property. The *in vitro* stability of [^{68}Ga]Ga-DOTAGA-RAMEB and the [$^{205/206}$Bi]Bi-DOTAGA-RAMEB was analyzed by analytical radio-HPLC in mouse serum at 37 °C. Samples were taken at 30, 60, and 90 min. Both compound: [^{68}Ga]Ga-DOTAGA-RAMEB and [$^{205/206}$Bi]Bi-DOTAGA-RAMEB remained stable over the measured time interval, with radiochemical purity exceeding 98 %. *In vivo* stability was tested in urine collected from mice 60 min after administration of the radiotracer. Neither [^{68}Ga]Ga-DOTAGA-RAMEB nor [$^{205/206}$Bi]Bi-DOTAGA-RAMEB showed measurable amounts of radioactive metabolite in the radio-HPLC results, which indicate excellent *in vivo* metabolic stability.

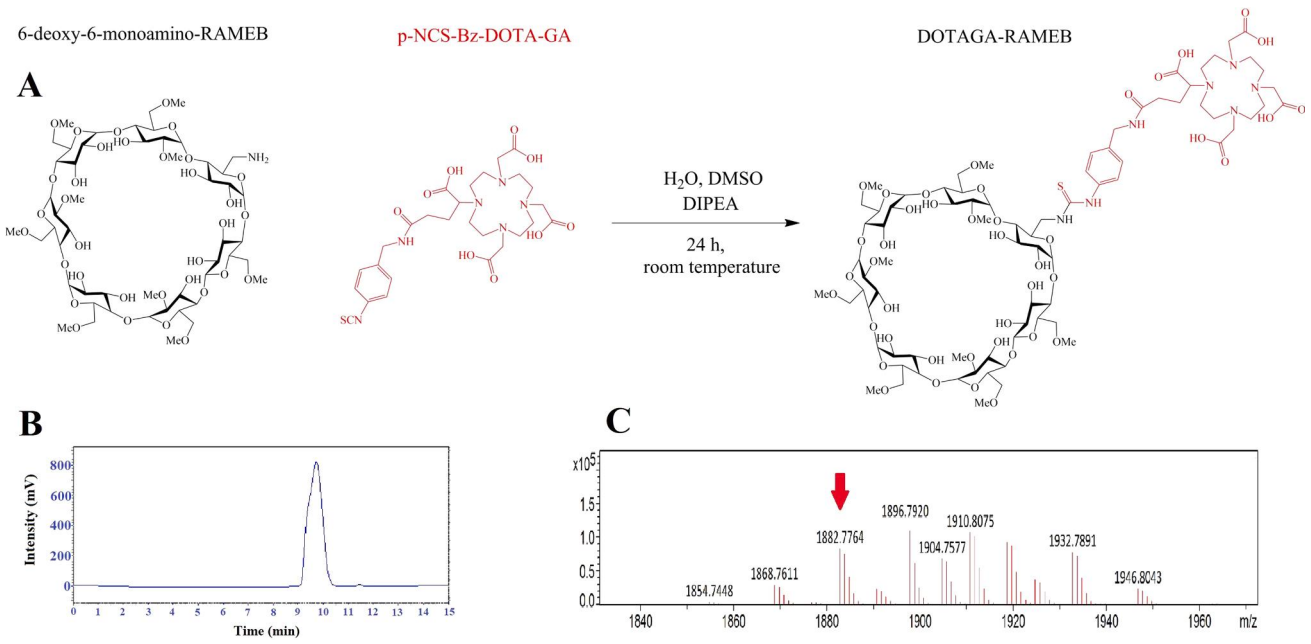

Fig. 1. Schematic representation of the synthesis (A), HPLC chromatogram (B) and mass spectrum (C) of the DOTAGA-RAMEB precursor.

3.4. In vivo evaluation of [^{68}Ga]Ga-DOTAGA-RAMEB biodistribution in healthy control mice

With the aim of assessing biological distribution of [^{68}Ga]Ga-DOTAGA-RAMEB dynamic PET imaging and *ex vivo* examinations were performed in healthy control CB17 SCID mice. Fig. 3 demonstrates representative dynamic PET images and average time-activity curve (TAC) after the intravenous injection of radiolabeled probe. Although, both the kidneys and the urinary bladder filled with urine could be directly visualized by qualitatively analysing the decay-corrected PET images, in other organs and tissues faint radiopharmaceutical accumulation could be depicted (Fig. 3A). Ninety minutes postinjection measurable radioactivity could only be detected in the kidney and in the bladder, background activity was not found. After 5 min, the tracer uptake of the examined tissues notably decreased, and 90 min after the injection the thoracic organs (pulmonary SUV_{mean}: 0.21 ± 0,05, heart SUV_{mean}: 0.38 ± 0.08) and the abdominal regions (intestinal SUV_{mean}:0.25 ± 0,06, liver SUV_{mean}: 0.25 ± 0.06, stomach SUV_{mean}: 0.14 ± 0.03) could only be featured with very low [^{68}Ga]Ga-DOTAGA-RAMEB accumulation. However, urinary radioactivity increased significantly 5 and 90 min postinjection with SUV_{mean} values of 3.93 ± 1.85 and 11.46 ± 2.75, respectively.

3.5. In vivo assessment of [^{68}Ga]Ga-DOTAGA-RAMEB biodistribution in BxPC-3 tumor-bearing mice

During the next part of our study the tumor targeting potential of [^{68}Ga]Ga-DOTAGA-RAMEB was defined using *in vivo* PET imaging approximately 12 days after the subcutaneous injection of PGE2 positive BxPC-3 cancer cells (Fig. 4). By the qualitative image analysis we found that the BxPC-3 tumors were clearly identified in the PET images using the [^{68}Ga]Ga-DOTAGA-RAMEB radiopharmaceutical (Fig. 4A). After the quantitative analysis of the decay-corrected PET images we found that from the 3rd minute (SUV_{mean}: 0.36 ± 0.04) post injection SUVmean values of BxPC-3 tumors were depicted to show a continuous decrease until the 50th minute (SUV_{mean}: 0.20 ± 0.04), then an equilibrium state has been reached (as shown in Fig. 4B). Based on these data we draw the conclusion that tumor-to-background (muscle) ratio, which is of remarkable importance regarding the evaluation of PET images was the highest 90 min after the injection of [^{68}Ga]Ga-DOTAGA-RAMEB, when T/M ratio was detected to be 2.5 ± 0.2 (Fig. 4B).

3.6. Ex vivo biodistribution analysis of [^{68}Ga]Ga-DOTAGA-RAMEB and [$^{205/206}$Bi]Bi-DOTAGA-RAMEB in BxPC-3 tumor-bearing mice

Table 1 and Fig. 5 demonstrates the results of *ex vivo* organ biodistribution examinations. PGE2 positive tumor-bearing BxPC-3 mice were dissected 30, 60 and 90 min after the injection of the radiopharmaceuticals and the radioactivity of the organs and the tissues were determined by gamma-counter. Statistically no significant difference was found between the %ID/g values of the examined organs and tissues in case of either radiotracers 30 and 60 min post injection, as shown in Fig. 5 and in the mentioned table. 90 min after the injection of [^{68}Ga]Ga-DOTAGA-RAMEB low concentration levels were detected in the examined organs and tissues. In contrast, [$^{205/206}$Bi]Bi-DOTAGA-RAMEB showed high uptake in the spleen, colon, stomach and in adipose tissue at the same investigation time point (Fig. 5). By analyzing the accumulation of [^{68}Ga]Ga-DOTAGA-RAMEB and [$^{205/206}$Bi]Bi-DOTAGA-RAMEB in the prostaglandin E2 positive BxPC-3 tumors, it was found that there was no significant ($P \leq 0.05$) difference between the two radiopharmaceuticals at any investigated time points.

3.7. Immunohistochemistry

The presence of PGE2 receptor of subcutaneously growing BxPC-3 tumors was verified applying immunohistochemical methods (Fig. 6). Strong receptor positivity characterized the tumors both in the cytoplasm and in the cell membrane. These results - in line with the *ex vivo* and *in vivo* examinations – strengthens the high binding affinity of [^{68}Ga]Ga-DOTAGA-RAMEB and [$^{205/206}$Bi]Bi-DOTAGA-RAMEB to PGE2 receptor.

4. Discussion

In recent years, the role of the prostaglandin E2 (PGE2) molecule and its receptors are receiving increasing attention in the field of experimental and clinical oncology. PGE2 is known to enhance the proliferation of tumor cells by promoting neoangiogenesis in tumors as well as anti-tumor immunity and inhibiting apoptosis (Liu et al., 2015; Wang and Dubois, 2006). However, it is known PGE2 is also a prognostic

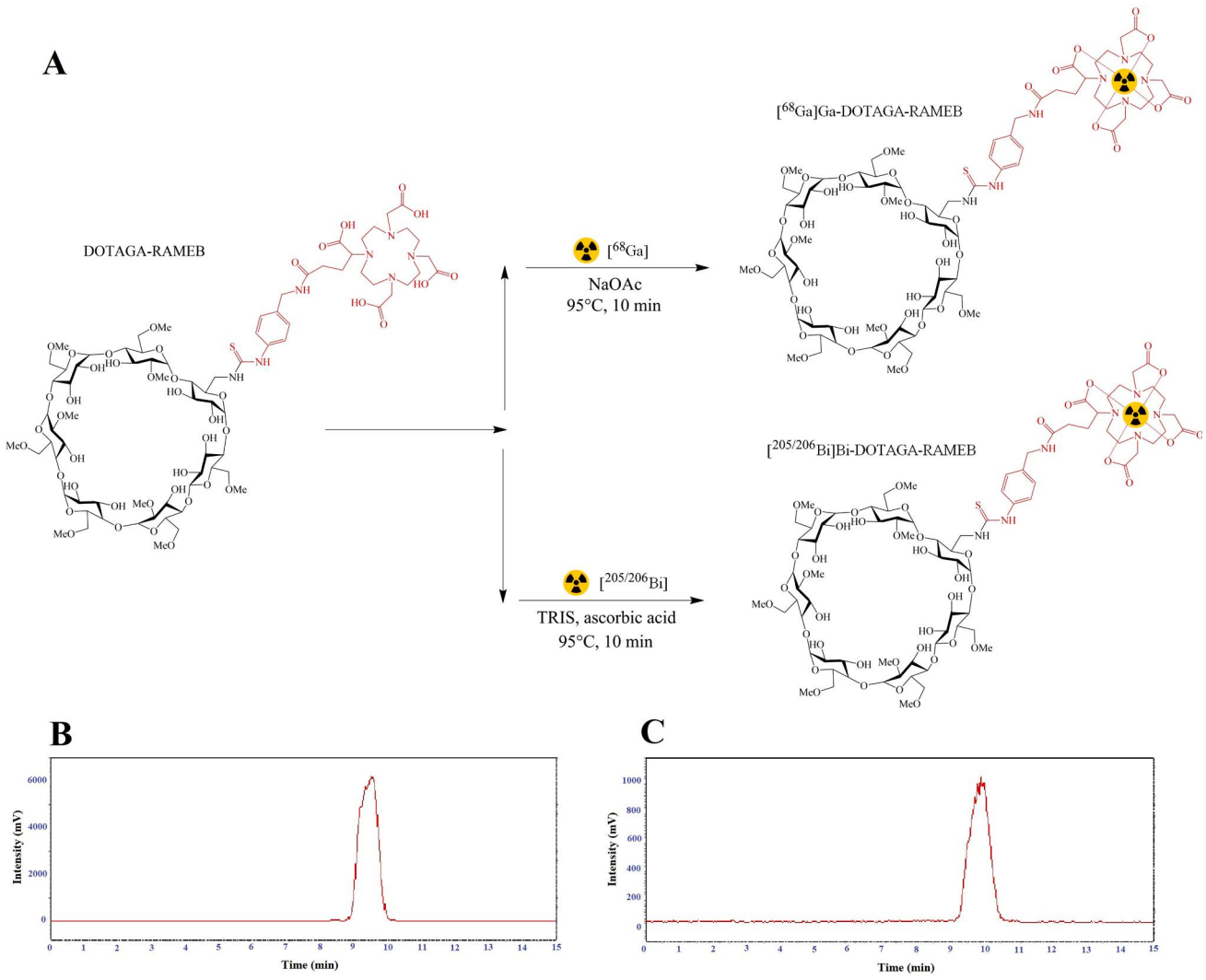

Fig. 2. Schematic representation of ^{68}Ga and $^{205/206}$Bi radiolabeling reactions of the DOTAGA-RAMEB precursor (A), Radio-HPLC chromatogram of the [^{68}Ga]Ga-DOTAGA-RAMEB (B), Radio-HPLC chromatogram of the [$^{205/206}$Bi]Bi-DOTAGA-RAMEB (C).

biomarker of various tumors (pancreatic, renal, oral, and breast cancers) (Tong et al., 2018). For these reasons it may play an important role in the *in vivo* diagnosis of PGE2-positive tumors by positron emission tomography and as a therapeutic target in the treatment of tumors.

Trencsényi and his research group in 2020 described that the random-methylated-β-cyclodextrin (RAMEB), binds with high affinity to PGE2-positive tumors. In their preclinical experiments, the RAMEB molecule was modified with NODAGA chelator and was radiolabeled with Gallium-68 positron-emitting radioisotope, and the resulting ^{68}Ga-NODAGA-RAMEB radiotracer was investigated in PGE2 positive tumor model using positron emission tomography. These results established the basis of PGE2-targeted *in vivo* PET diagnostics (Trencsényi et al., 2020). Based on our previous results, we aimed to synthesize a RAMEB cyclodextrin derivative that binds with high affinity to PGE2-positive tumors and can be radiolabeled with both diagnostic and therapeutic isotopes.

For this reason, the DOTAGA chelator was chosen for the synthesis of ^{68}Ga and $^{205/206}$Bi-labeled radiopharmaceuticals (Bernhard et al., 2012; Okoye et al., 2019). DOTA and their derivatives represent a significant group of complexing agents in biomedical applications due to their excellent complexing properties against many metal ions and the high kinetic stability of their metal complexes (Lattuada et al., 2011; Wadas et al., 2010). In this study DOTAGA bifunctional chelator was conjugated via the amino group of NH_2-RAMEB (Okoye et al., 2019) (Fig. 1) DOTAGA contains four free acidic groups and an activated group, which was able to react specifically with an amino group (Levy et al., 2009; Overoye-Chan et al., 2008). For these types of bifunctional chelators that contain a pentafluorophenyl ester or succinimidyl ester group, no protection/deprotection reactions and time-consuming chromatographic work are required. The in this way newly synthesized DOTAGA-RAMEB is suitable for radiolabeling with both ^{68}Ga (Anderson and McAnulty, 2013; Filippi et al., 2020) and $^{205/206}$Bi (Suthiram et al., 2021) isotopes.

Radiolabeling procedures were performed according to well-established protocols, similar to our previous work (Hajdu et al., 2019; Trencsényi et al., 2020), resulting in products with high radiochemical purity (above 98.0 %) (Fig. 2). In case of ^{68}Ga labeling generator was eluted with ultra pure HCl (c = 0.1 M, pH = 1). The strongly acidic milieu (pH < 2) is inadequate for radiolabeling, therefore the eluates were buffered using 1 M sodium acetate to provide a pH of 4.3–4.5. (Hacht, 2008; Tsionou et al., 2017) In all preparations, the ^{68}Ga-eluate was buffered and was added directly to the DOTAGA-RAMEB which resulted an efficient robust radiolabeling reaction. In case of $^{205/206}$Bi labeling the radiolabeling reaction must be done at a pH of 8.2–8.5. This pH values reducing precipitation of bismuth hydroxide and results an effective labeling reaction (Egorova et al., 2018; Manna et al., 2020). In this case the $^{205/206}$Bi-solution was added directly to a pre-buffered DOTAGA-RAMEB precursor.

The applicability of our radiolabeled products was then evaluated by

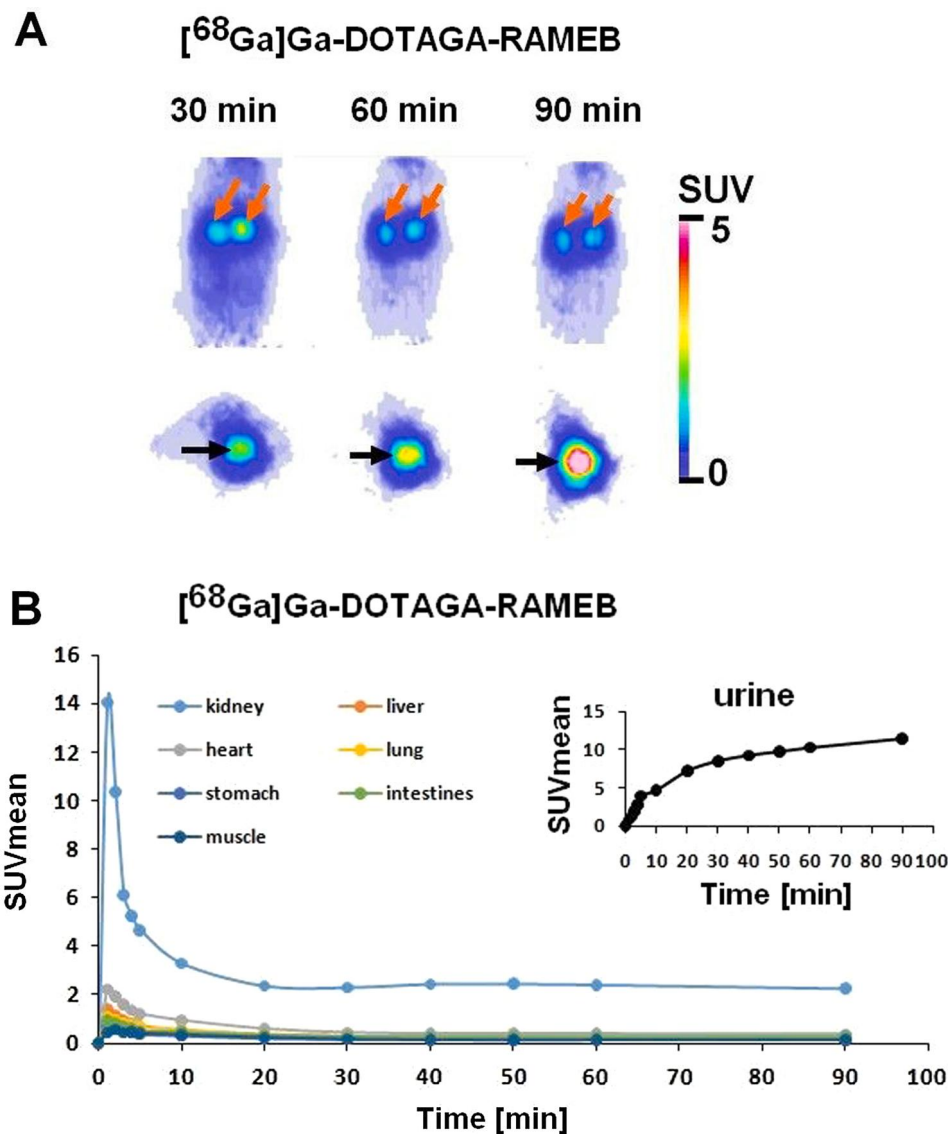

Fig. 3. *In vivo* biodistribution of intravenously injected [^{68}Ga]Ga-DOTAGA-RAMEB in healthy control SCID mice. Representative decay-corrected dynamic PET images (A) and time-activity curve (B) of [^{68}Ga]Ga-DOTAGA-RAMEB in selected organs and tissues of healthy SCID mice. Orange arrows: kidneys; black arrows: bladder. (For interpretation of the references to colour in this figure legend, the reader is referred to the web version of this article.)

in vitro and *in vivo* stability tests. The *in vitro* metabolic stability was monitored after 30, 60 and 90 min incubation time, based on our previous studies (Hajdu et al., 2019; Trencsényi et al., 2020), because this interval corresponds to the time residence of the tracer in the body. The stability test showed there were no ^{68}Ga and $^{205/206}$Bi isotopes leakage or tracer fragmentation during the 90 min investigation time period. Results demonstrated that the ^{68}Ga and $^{205/206}$Bi labeled derivatives were stable in the presence of serum, similarly to our previous compounds, which is important for intravenous administration. *In vivo* metabolic stability was evaluated 60 min after intravenous administration of radiotracers. As no radioactive metabolite was found in the urine, it was determined that the *in vivo* stability results are consistent with the *in vitro* data. These experimental results demonstrated that the newly prepared [^{68}Ga]Ga-DOTAGA-RAMEB and [$^{205/206}$Bi]Bi-DOTAGA-RAMEB are stable during the circulation and excretion, which is essential for further *in vivo* experiments.

During the determination of partition coefficient, it was found that the log*P* value of ^{68}Ga-labeled derivative was -3.47 ± 0.04, and the $^{205/206}$Bi-labeled derivative was -3.45 ± 0.03 suggesting that these tracers are highly hydrophilic.

In the first of the preclinical studies, biodistribution of [^{68}Ga]Ga-DOTAGA-RAMEB was determined in healthy control CB17 SCID mice applying *in vivo* PET imaging (Fig. 3). Urinary excretion of [^{68}Ga]Ga-DOTAGA-RAMEB could be visualized on the decay-corrected PET images. Average log*P* values of -3.5 indicating highly hydrophilic property could underpin this observation. This result is consistent with the biodistribution data of [^{68}Ga]Ga-NODAGA-RAMEB previously examined by our research group, where renal excretion was revealed as well according to the log*P* values (Trencsényi et al., 2020). As for other organs and tissues, low tracer accumulation was depicted by *in vivo* PET imaging both in case of the previously examined [^{68}Ga]Ga-NODAGA-RAMEB and [^{68}Ga]Ga-DOTAGA-RAMEB produced by the exchange of the chelator. Time-activity curves demonstrate rapid tracer clearance (Fig. 3B). Our elimination results are in line with the outcomes of experiments with other types of cyclodextrins (HPβCD) done by different laboratories, which reported renal excretion during similar examinations on humans and rodents performed with unlabeled and radiolabeled HPβCD (Hajdu et al., 2019).

During the second phase of the preclinical research, tumor-targeting capability of [^{68}Ga]Ga-DOTAGA-RAMEB was assessed in PGE2-positive

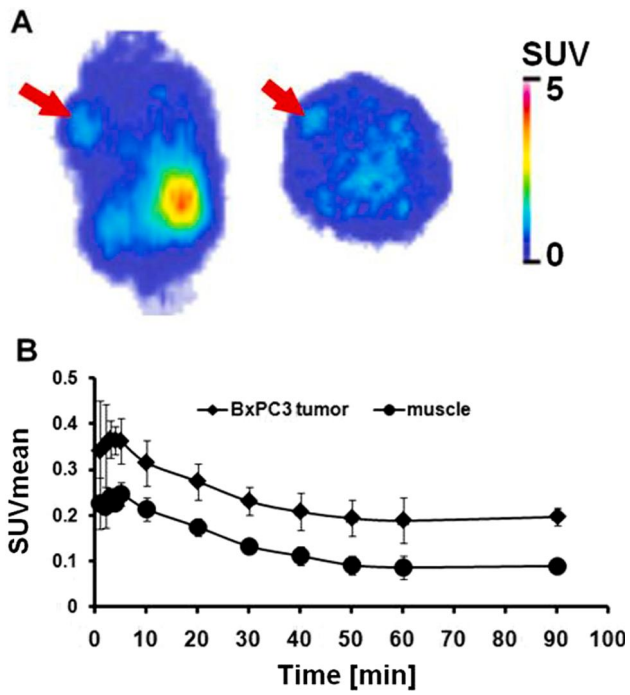

Fig. 4. *In vivo* biodistribution of the intravenously injected [^{68}Ga]Ga-DOTAGA-RAMEB in BxPC-3 tumor-bearing SCID mice. Panel A: Representative decay-corrected static coronal (left) and transaxial (right) PET images 90 min after radiotracer injection. Panel B: Time-activity curve (B) of [^{68}Ga]Ga-DOTAGA-RAMEB in BxPC-3 tumor and muscle (background). Red arrows: subcutaneously growing BxPC-3 tumor. (For interpretation of the references to colour in this figure legend, the reader is referred to the web version of this article.)

tumor-bearing mice by *in vivo* PET imaging. Already confirmed by other research teams, PGE2 overexpression and EP2 receptor upregulation characterized those BxPC-3 cancerous cells that were used in our experiments (Takahashi et al., 2015). We also verified the presence of PGE2 receptors of subcutaneously growing BxPC-3 tumors applying immunohistochemical methods (Fig. 6). Due to the strong receptorial overexpression tumors could be accurately localized by *in vivo* PET imaging after the intravenous injection of [^{68}Ga]Ga-DOTAGA-RAMEB (Fig. 4). Highest T/M ratio (2.5 ± 0.2) could be experienced 90 min post injection, which is of considerable significance regarding the evaluation of PET images. Comparing this with our previous examinations using BxPC-3 tumors, the highest tumor-to-background ratio was also observed at 80–90 min post injection (Trencsényi et al., 2020). Summarizing the results of *in vivo* imaging, we concluded that the exchange of the chelator NODAGA for DOTAGA did not influence either the biological behavior of ^{68}Ga-labeled RAMEB or its PGE2-positive tumor-targeting ability.

Since due to its physical characteristic features $^{205/206}$Bi could not be detected by PET scanner, the comparative analysis of the accumulation of [^{68}Ga]Ga-DOTAGA-RAMEB and [$^{205/206}$Bi]Bi-DOTAGA-RAMEB was performed using a gamma counter. Based on the %ID/g results of the *ex vivo* experiments, no statistically significant difference was detected between the %ID/g values of the examined organs and tissues 30 and 60 min after the injection in case of either radiotracers (seen on Fig. 5 and Table 1). As for some organs, the uptake of the two radiopharmaceuticals differed at 90th minutes post injection. The [^{68}Ga]Ga-DOTAGA-RAMEB accumulation was low in the given organs at this time of measurement. These data are in accordance with the results of *in vivo* PET studies and those of previous research with [^{68}Ga]Ga-NODAGA-RAMEB and [^{68}Ga]Ga-NODAGA-HPβCD (Hajdu et al., 2019; Trencsényi et al., 2020). Conversely, intensive accumulation of [$^{205/206}$Bi]Bi-DOTAGA-RAMEB was noticed in the spleen, colon, and adipose tissue, that could not be explained by the −3.45 log*P* value of the molecule. Although, physicochemical features of $^{205/206}$Bi may underpin our result, large scale future studies are required for the correct interpretation of this finding. Considering the tumor-targeting capability of the tracers, we revealed that both [^{68}Ga]Ga-DOTAGA-RAMEB and [$^{205/206}$Bi]Bi-DOTAGA-RAMEB were taken up by PGE2-positive BxPC-3 neoplasms and no remarkable difference was experienced between the %ID/g values of the two radiopharmaceuticals at either time of the analysis ($p \leq 0.05$).

5. Conclusions

Both newly synthesized [^{68}Ga]Ga-DOTAGA-RAMEB and [$^{205/206}$Bi]Bi-DOTAGA-RAMEB showed specific binding in PGE2-positive BxPC-3 tumors. Due to its high selectivity and rapid elimination, [^{68}Ga]Ga-

Table 1
Ex vivo biodistribution of [^{68}Ga]Ga-DOTAGA-RAMEB and [$^{205/206}$Bi]Bi-DOTAGA-RAMEB radiotracers 30, 60 and 90 min after injection. %ID/g tissue data is expressed as mean ± SD.

	[^{68}Ga] Ga-DOTAGA-RAMEB 30 min (n = 5)	**[^{68}Ga] Ga-DOTAGA-RAMEB 60 min** (n = 5)	**[^{68}Ga] Ga-DOTAGA-RAMEB 90 min** (n = 5)	**[$^{205/206}$Bi] Bi-DOTAGA-RAMEB 30 min** (n = 5)	**[$^{205/206}$Bi] Bi-DOTAGA-RAMEB 60 min** (n = 5)	**[$^{205/206}$Bi] Bi-DOTAGA-RAMEB 90 min** (n = 5)
blood	0.80 ± 0.04	0.27 ± 0.03	0.14 ± 0.02	0.53 ± 0.37	0.25 ± 0.08	0.19 ± 0.16
liver	0.25 ± 0.09	0.14 ± 0.04	0.10 ± 0.01	0.29 ± 0.25	0.11 ± 0.01	0.10 ± 0.06
spleen	0.33 ± 0.08	0.18 ± 0.01	0.09 ± 0.01	0.55 ± 0.62	0.19 ± 0.05	0.49 ± 0.46
kidney	3.27 ± 0.86	1.39 ± 0.19	1.54 ± 0.09	3.71 ± 2.86	2.02 ± 0.21	2.42 ± 0.13
small intestine	0.19 ± 0.02	0.06 ± 0.01	0.04 ± 0.01	0.21 ± 0.12	0.10 ± 0.02	0.15 ± 0.17
large intestine	0.45 ± 0.17	0.15 ± 0.01	0.10 ± 0.04	0.44 ± 0.38	0.15 ± 0.14	0.92 ± 1.47
stomach	0.39 ± 0.22	0.13 ± 0.03	0.13 ± 0.11	0.31 ± 0.12	0.12 ± 0.04	0.42 ± 0.31
muscle	0.16 ± 0.06	0.04 ± 0.01	0.02 ± 0.01	0.21 ± 0.20	0.04 ± 0.02	0.04 ± 0.04
fat	0.77 ± 0.18	0.07 ± 0.01	0.08 ± 0.01	0.27 ± 0.18	0.07 ± 0.02	0.18 ± 0.18
lung	0.83 ± 0.16	0.32 ± 0.01	0.15 ± 0.12	0.64 ± 0.29	0.38 ± 0.02	0.25 ± 0.14
heart	0.30 ± 0.02	0.11 ± 0.01	0.06 ± 0.01	0.27 ± 0.23	0.10 ± 0.05	0.11 ± 0.09
brain	0.57 ± 0.01	0.01 ± 0.01	0.01 ± 0.01	0.02 ± 0.03	0.01 ± 0.01	0.01 ± 0.01
bone (femur)	0.19 ± 0.03	0.06 ± 0.01	0.03 ± 0.02	0.16 ± 0.12	0.10 ± 0.06	0.02 ± 0.03
salivary glands	0.20 ± 0.01	0.08 ± 0.01	0.06 ± 0.01	0.18 ± 0.11	0.09 ± 0.01	0.08 ± 0.06
gall bladder	0.61 ± 0.35	0.19 ± 0.08	0.09 ± 0.03	0.49 ± 0.70	0.42 ± 0.05	0.04 ± 0.03
pancreas	0.17 ± 0.04	0.06 ± 0.01	0.04 ± 0.01	0.21 ± 0.23	0.21 ± 0.04	0.12 ± 0.15
BxPC3 tumor	0.75 ± 0.25	0.31 ± 0.05	0.28 ± 0.11	0.64 ± 0.34	0.36 ± 0.04	0.21 ± 0.13

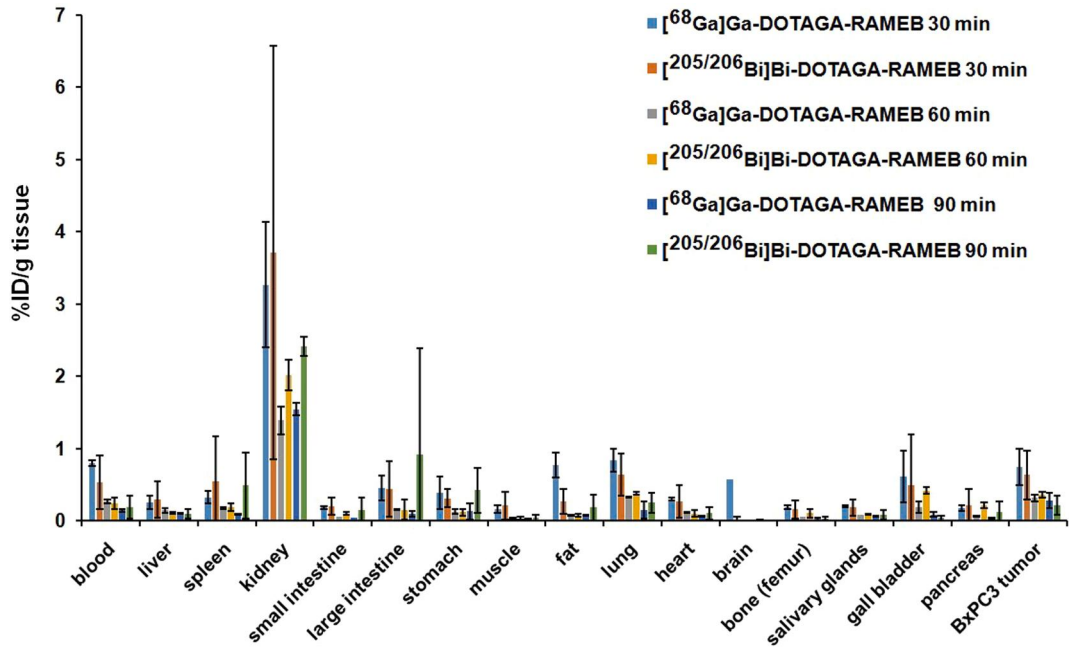

Fig. 5. *Ex vivo* biodistribution of [^{68}Ga]Ga-DOTAGA-RAMEB and [$^{205/206}$Bi]Bi-DOTAGA-RAMEB in PGE2 positive BxPC-3 tumor-bearing CB17 SCID mice (n = 5/time point/radiotracer) 30, 60 and 90 after radiotracer injection and 12 ± 1 days after tumor cell inoculation. %ID/g tissue data is expressed as mean ± SD.

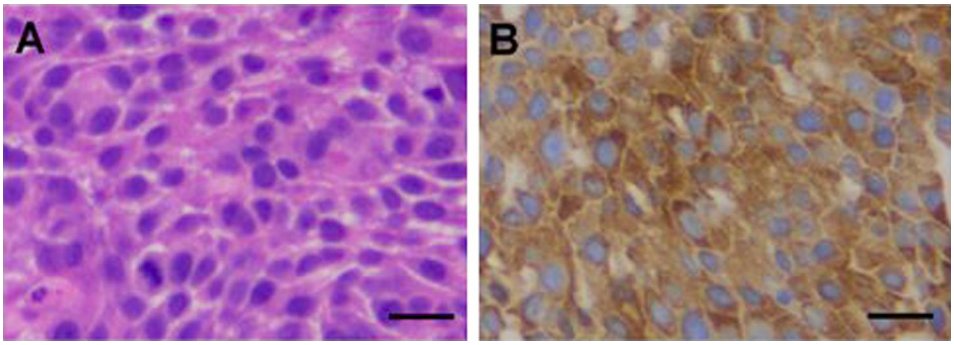

Fig. 6. Histological analysis of subcutaneously growing BxPC-3 tumors 12 days after the inoculation of tumor cells. A: hematoxylin-eosin staining; B: immunohistochemistry of Prostaglandin E receptor using EP2/PTGER2 antibody with 3,3-diaminobenzidine (DAB) (brown). Magnification: 40x. Bar: 50 μm.

DOTAGA-RAMEB seems to be a promising radiotracer in the PET diagnostics of PGE2-positive tumors. Furthermore, [$^{205/206}$Bi]Bi-DOTAGA-RAMEB, as a model compound of [^{213}Bi]Bi-DOTAGA-RAMEB, may promotes the biological studies and radiochemical developments in the field of radionuclide therapy of PGE2-positive malignancies.

CRediT authorship contribution statement

Katalin Csige: Writing – original draft. **Judit P. Szabó:** . **Ibolya Kálmán-Szabó:** . **Noémi S. Dénes:** Methodology. **Dezső Szikra:** . **Zita Képes:** Investigation, Data curation. **Gábor Opposits:** Software, Visualization. **Gábor Méhes:** Methodology. **István Kertész:** Methodology. **Ferenc Fenyvesi:** Conceptualization. **György Trencsényi:** Methodology. **István Hajdu:** Conceptualization, Supervision, Writing – review & editing.

Declaration of Competing Interest

The authors declare that they have no known competing financial interests or personal relationships that could have appeared to influence the work reported in this paper.

Data availability

Data will be made available on request.

Acknowledgements

This research was supported by the Thematic Excellence Programme (TKP2020-NKA-04) of the Ministry for Innovation and Technology in Hungary and by the János Bolyai Research Scholarship of the Hungarian Academy of Sciences (bo_328_21). PhD students were supported by the University of Debrecen, Doctoral School of Pharmaceutical Sciences and EFOP-3.6.3-VEKOP-16-2017-00009 grant.

References

Ahenkorah, S., Cassells, I., Deroose, C.M., Cardinaels, T., Burgoyne, A.R., Bormans, G., Ooms, M., Cleeren, F., 2021. Bismuth-213 for Targeted Radionuclide Therapy: From Atom to Bedside. Pharmaceutics 13, 599. https://doi.org/10.3390/pharmaceutics13050599.

Anderson, A., McAnulty, T. (Eds.), 2013. Somatostatin: synthesis, mechanisms-of-action and physiological effects, Endocrinology research and clinical developments. Nova Science Publishers, Inc, [Hauppauge?], New York.

Bernhard, C., Moreau, M., Lhenry, D., Goze, C., Boschetti, F., Rousselin, Y., Brunotte, F., Denat, F., 2012. DOTAGA-anhydride: a valuable building block for the preparation

of DOTA-like chelating agents. Chemistry 18, 7834–7841. https://doi.org/10.1002/chem.201200132.
Del Valle, E.M.M., 2004. Cyclodextrins and their uses: a review. Process Biochem. 39, 1033–1046. https://doi.org/10.1016/S0032-9592(03)00258-9.
Egorova, B.V., Matazova, E.V., Mitrofanov, A.A., Aleshin, G.Y., Trigub, A.L., Zubenko, A. D., Fedorova, O.A., Fedorov, Y.V., Kalmykov, S.N., 2018. Novel pyridine-containing azacrownethers for the chelation of therapeutic bismuth radioisotopes: Complexation study, radiolabeling, serum stability and biodistribution. Nucl Med Biol 60, 1–10. https://doi.org/10.1016/j.nucmedbio.2018.01.005.
Filippi, L., Pizzichini, P., Bagni, O., Scopinaro, F., 2020. Somatostatin Receptor Analogs. In: Calabria, F., Schillaci, O. (Eds.), Radiopharmaceuticals. Springer International Publishing, Cham, pp. 99–113. https://doi.org/10.1007/978-3-030-27779-6_6.
Frijlink, H.W., Visser, J., Hefting, N.R., Oosting, R., Meijer, D.K., Lerk, C.F., 1990. The pharmacokinetics of beta-cyclodextrin and hydroxypropyl-beta-cyclodextrin in the rat. Pharm Res 7, 1248–1252. https://doi.org/10.1023/a:1015929720063.
Hacht, B., 2008. Gallium(III) Ion Hydrolysis under Physiological Conditions. Bull. Korean Chem. Soc. 29, 372–376. https://doi.org/10.5012/BKCS.2008.29.2.372.
Hajdu, I., Angyal, J., Szikra, D., Kertész, I., Malanga, M., Fenyvesi, É., Szente, L., Vecsernyés, M., Bácskay, I., Váradi, J., Fehér, P., Ujhelyi, Z., Vasvári, G., Rusznyák, Á., Trencsényi, G., Fenyvesi, F., 2019. Radiochemical synthesis and preclinical evaluation of 68Ga-labeled NODAGA-hydroxypropyl-beta-cyclodextrin (68Ga-NODAGA-HPBCD). Eur. J. Pharm. Sci. 128, 202–208. https://doi.org/10.1016/j.ejps.2018.12.001.
Kellerbauer, A., Bruchertseifer, F., Malmbeck, R., Morgenstern, A., 2020. Targeted α therapy with ^{213} Bi and ^{225} Ac. J. Phys.: Conf. Ser. 1643, 012205. https://doi.org/10.1088/1742-6596/1643/1/012205.
Kratochwil, C., Giesel, F.L., Bruchertseifer, F., Mier, W., Apostolidis, C., Boll, R., Murphy, K., Haberkorn, U., Morgenstern, A., 2014. ^{213}Bi-DOTATOC receptor-targeted alpha-radionuclide therapy induces remission in neuroendocrine tumours refractory to beta radiation: a first-in-human experience. Eur J Nucl Med Mol Imaging 41, 2106–2119. https://doi.org/10.1007/s00259-014-2857-9.
Lattuada, L., Barge, A., Cravotto, G., Giovenzana, G.B., Tei, L., 2011. The synthesis and application of polyamino polycarboxylic bifunctional chelating agents. Chem Soc Rev 40, 3019–3049. https://doi.org/10.1039/c0cs00199f.
Levy, S.G., Jacques, V., Zhou, K.L., Kalogeropoulos, S., Schumacher, K., Amedio, J.C., Scherer, J.E., Witowski, S.R., Lombardy, R., Koppetsch, K., 2009. Development of a Multigram Asymmetric Synthesis of 2-(*R*)-2-(4,7,10-Tris *tert* -Butylcarboxymethyl-1,4,7,10-tetraazacyclododec-1-yl)-pentanedioic Acid, 1- *tert* -Butyl Ester, (*R*)- *tert* -Bu $_4$ -DOTAGA. Org. Process Res. Dev. 13, 535–542. https://doi.org/10.1021/op8002932.
Liu, B., Qu, L., Yan, S., 2015. Cyclooxygenase-2 promotes tumor growth and suppresses tumor immunity. Cancer Cell Int 15, 106. https://doi.org/10.1186/s12935-015-0260-7.
Manna, P., Szücs, D., Csupász, T., Fekete, A., Szikra, D., Lin, Z., Gáspár, A., Bhattacharya, S., Zulaica, A., Tóth, I., Kortz, U., 2020. Shape and Size Tuning of Bi ^{III} -Centered Polyoxopalladates: High Resolution ^{209} Bi NMR and $^{205/206}$ Bi Radiolabeling for Potential Pharmaceutical Applications. Inorg. Chem. 59, 16769–16782. https://doi.org/10.1021/acs.inorgchem.0c02857.
Morgenstern, A., Bruchertseifer, F., Apostolidis, C., 2012. Bismuth-213 and actinium-225 – generator performance and evolving therapeutic applications of two generator-derived alpha-emitting radioisotopes. Curr Radiopharm 5, 221–227. https://doi.org/10.2174/1874471011205030221.
Nelson, B.J.B., Andersson, J.D., Wuest, F., 2020. Targeted Alpha Therapy: Progress in Radionuclide Production, Radiochemistry, and Applications. Pharmaceutics 13, 49. https://doi.org/10.3390/pharmaceutics13010049.
Norenberg, J.P., Krenning, B.J., Konings, I.R.H.M., Kusewitt, D.F., Nayak, T.K., Anderson, T.L., de Jong, M., Garmestani, K., Brechbiel, M.W., Kvols, L.K., 2006. 213Bi-[DOTA0, Tyr3]octreotide peptide receptor radionuclide therapy of pancreatic tumors in a preclinical animal model. Clin Cancer Res 12, 897–903. https://doi.org/10.1158/1078-0432.CCR-05-1264.
O'Callaghan, G., Houston, A., 2015. Prostaglandin E2 and the EP receptors in malignancy: possible therapeutic targets? Br J Pharmacol 172, 5239–5250. https://doi.org/10.1111/bph.13331.
Okoye, N.C., Baumeister, J.E., Najafi Khosroshahi, F., Hennkens, H.M., Jurisson, S.S., 2019. Chelators and metal complex stability for radiopharmaceutical applications. Radiochim. Acta 107, 1087–1120. https://doi.org/10.1515/ract-2018-3090.
Ottinger, E.A., Kao, M.L., Carrillo-Carrasco, N., Yanjanin, N., Shankar, R.K., Janssen, M., Brewster, M., Scott, I., Xu, X., Cradock, J., Terse, P., Dehdashti, S.J., Marugan, J., Zheng, W., Portilla, L., Hubbs, A., Pavan, W.J., Heiss, J., Vite, C.H., Walkley, S.U., Ory, D.S., Silber, S.A., Porter, F.D., Austin, C.P., McKew, J.C., 2014. Collaborative development of 2-hydroxypropyl-β-cyclodextrin for the treatment of Niemann-Pick type C1 disease. Curr Top Med Chem 14, 330–339. https://doi.org/10.2174/1568026613666131127160118.
Overoye-Chan, K., Koerner, S., Looby, R.J., Kolodziej, A.F., Zech, S.G., Deng, Q., Chasse, J.M., McMurry, T.J., Caravan, P., 2008. EP-2104R: A Fibrin-Specific Gadolinium-Based MRI Contrast Agent for Detection of Thrombus. J. Am. Chem. Soc. 130, 6025–6039. https://doi.org/10.1021/ja800834y.
Reader, J., Holt, D., Fulton, A., 2011. Prostaglandin E2 EP receptors as therapeutic targets in breast cancer. Cancer Metastasis Rev 30, 449–463. https://doi.org/10.1007/s10555-011-9303-2.
Suthiram, J., Ebenhan, T., Marjanovic-Painter, B., Sathekge, M.M., Zeevaart, J.R., 2021. Towards Facile Radiolabeling and Preparation of Gallium-68-/Bismuth-213-DOTA-[Thi8, Met(O2)11]-Substance P for Future Clinical Application: First Experiences. Pharmaceutics 13, 1326. https://doi.org/10.3390/pharmaceutics13091326.
Takahashi, T., Uehara, H., Ogawa, H., Umemoto, H., Bando, Y., Izumi, K., 2015. Inhibition of EP2/EP4 signaling abrogates IGF-1R-mediated cancer cell growth: involvement of protein kinase C-θ activation. Oncotarget 6, 4829–4844. https://doi.org/10.18632/oncotarget.3104.
Tong, D., Liu, Q., Wang, L.-A., Xie, Q., Pang, J., Huang, Y., Wang, L., Liu, G., Zhang, D., Lan, W., Jiang, J., 2018. The roles of the COX2/PGE2/EP axis in therapeutic resistance. Cancer Metastasis Rev 37, 355–368. https://doi.org/10.1007/s10555-018-9752-y.
Trencsényi, G., Kis, A., Szabó, J.P., Ráti, Á., Csige, K., Fenyvesi, É., Szente, L., Malanga, M., Méhes, G., Emri, M., Kertész, I., Vecsernyés, M., Fenyvesi, F., Hajdu, I., 2020. In vivo preclinical evaluation of the new 68Ga-labeled beta-cyclodextrin in prostaglandin E2 (PGE2) positive tumor model using positron emission tomography. Int J Pharm 576, 118954. https://doi.org/10.1016/j.ijpharm.2019.118954.
Tsionou, M.I., Knapp, C.E., Foley, C.A., Munteanu, C.R., Cakebread, A., Imberti, C., Eykyn, T.R., Young, J.D., Paterson, B.M., Blower, P.J., Ma, M.T., 2017. Comparison of macrocyclic and acyclic chelators for gallium-68 radiolabelling. RSC Adv. 7, 49586–49599. https://doi.org/10.1039/C7RA09076E.
Wadas, T.J., Wong, E.H., Weisman, G.R., Anderson, C.J., 2010. Coordinating radiometals of copper, gallium, indium, yttrium, and zirconium for PET and SPECT imaging of disease. Chem Rev 110, 2858–2902. https://doi.org/10.1021/cr900325h.
Wang, D., Dubois, R.N., 2006. Prostaglandins and cancer. Gut 55, 115–122. https://doi.org/10.1136/gut.2004.047100.